INSTITUTE OF PLASMA PHYSICS

NAGOYA UNIVERSITY

Boundary Conditions for a Simulation Plasma in a Magnetic Field

H. Naitou, S. Tokuda* and T. Kamimura

IPPJ- 307

September 1977

RESEARCH REPORT

NAGOYA, JAPAN

On Boundary Conditions for a Simulation Plasma in a Magnetic Field

H. Naitou, S. Tokuda* and T. Kamimura

IPPJ- 307 September 1977

Further communication about this report is to be sent to the Research Information Center, Institute of Plasma Physics, Nagoya University, Nagoya, Japan

---

* Plasma Physics Research Laboratory, Faculty of Engineering, Osaka University, Osaka 565, Japan.

Abstract

Different treatments of the particles at the boundary wall in a magnetized and bounded simulation plasma are studied extensively. It is shown that Lee and Okuda's boundary conditions are numerically unstable. The existence of drift wave like instability at the boundary is verified numerically. Methods to eliminate this surface instability are presented, which do not produce any density gradients or surface currents at the boundary.

§1. Introduction

Particle simulation has contributed to the understandings of plasma physics. In particular it is a powerful tool for understanding transport phenomena across a magnetic field. Plasma diffusion due to low frequency convective cells[1] and electron diffusion caused by low frequency ion fluctuations or lower hybrid waves[2] are some examples.

In many of these, the infinite and homogeneous plasma is simulated by using periodic boundary conditions. There are no numerical difficulty with these boundary conditions. However all experimental plasmas are finite and bounded, and hence inhomogeneous. Inhomogenities in plasmas produce many interesting phenomena, for example drift wave instabilities and trapped particle instabilities. It is important to use a bounded plasma model to simulate a inhomogeneous plasma. Moreover bounded plasma model itself involves many significant phenomena; Gould Trivelpiece waves[3], sheath layers and their oscillations[4] etc.

Boundary conditions for a bounded simulation plasma have not been studied extensively.[5-7] Owing to the restrictions on memory and CPU time for computers, we can only simulate a small volume of plasma compared with real one. Further we must determine the boundary conditions in such a way so as not to disturb the phenomena of interest in the interior of the plasma. If one is not careful, the boundary phenomena can dominate the whole plasma.

The important boundary condition for simulating a bounded plasma in a static external magnetic field is the treatment of particles at plane walls which are parallel to the magnetic field. These boundaries modify the cyclotron motion of charged particles and cause shifts of guiding centers of particles which hit the walls, macroscopic density gradients, currents near the boundaries and surface waves etc. These effects seriously violate the simulation of plasma phenomena of interest.

W.W. Lee and H. Okuda[5] examined the above mentioned boundary effects and conclude that the noise produced by the plasma boundary interactions mainly comes from the disturbance of the guiding center positions of the particles which hit the walls. They have used a rather artificial boundary condition in which the positions of the guiding centers of the particles striking the wall are not changed.

We have performed a simulation using Lee and Okuda's boundary condition with uniform density and temperature profiles using a 2 - 1/2 dimensional (2 positions and 3 velocities) particle code and found that there is a strong instability around the boundary. This surface instability, which is quite similar to the drift wave instability driven by the density gradients, considerably affects the entire plasma because in the nonlinear stage it spreads beyond a distance of one ion Larmor diameter from the boundary. Therefore the main aim of this paper is to develop boundary conditions which introduce no surface instability.

In Sec.2, the method used by Lee and Okuda is discussed and the surface instability produced by their method is demonstrated. In Sec.3, methods which eliminate the surface instability are presented. Comparisons with other methods are also discussed. Concluding remarks and discussions are given in Sec.5.

§2. Lee and Okuda's method and the surface instability

First we review the method of treating particles at the boundary proposed by W.W. Lee and H. Okuda[5] (we will call this LOM). They used LOM in their simulations of drift waves.[8-10] For simplicity let us think of a 2 dimensional (2 positions and 2 velocities) electrostatic plasma which is normal to the magnetic field and periodic in the y direction but bounded by walls at x=0 and $x=L_x$ with the potential equal to zero on these boundaries. This system corresponds to the case of $\theta=0°$ in Fig.2, where θ is the angle between the z axis and the direction of the magnetic field. We concentrate our attention on the wall at x=0.

Lee and Okuda claim that the reflecting boundary conditions, where a particle exiting from the system is reflected back into the original system at every time step with $x \to -x$ and $v_x \to -v_x$ (see Fig.1-a) causes two effects; (1) a sheath current along the wall and (2) a sharp density gradient near the boundary the width of which is of the order of a Larmor radius. These effects come from the disturbance of the guiding center positions of the particles which strike the wall. They modified the boundary condition and proposed the method LOM which is illustrated in Fig.1-b. In LOM, particles which hit the wall are reflected by the reflecting boundary condition but moved in a inversed magnetic field until they hit the wall again where they are reflected and moved in a normal magnetic field. It is to be noted that both the particles which move in a normal magnetic field and ones which move in a inversed magnetic field, feel the electric fields in their actual positions without changing the sign of their charge. The guiding centers of the particles do not change in LOM by the wall particle interactions. Total energy is conserved as well as the total charge. However they state that additional smoothings of the charge modulation in y direction before the reflections are sometimes necessary to minimize the noise.

The merit of LOM is that it produces no density gradient near the wall. However, it causes a macroscopic current in the y direction. We have the macroscopic density $n_\sigma^{LOM}(x)$ and velocity $\vec{v}_\sigma^{LOM}(x)$;

$$n_\sigma^{LOM}(x) = \text{const.}$$
$$\vec{v}_\sigma^{LOM}(x) = \text{sgn}(q_\sigma)\sqrt{\frac{2}{\pi}}\ v_{t\sigma}\ \exp[-\frac{x^2}{2\rho_\sigma{}^2}]\vec{i}_y \tag{1}$$

where q_σ, $\vec{v}_{t\sigma}$ and ρ_σ are the charge, the thermal velocity $(=\sqrt{T_\sigma/m_\sigma})$ and the Larmor radius $(=v_{t\sigma}/\omega_{c\sigma})$ for species σ $(\sigma=e,\ i)$ respectively, and $\vec{i}_y$ is the unit vector in the y direction. Eqs.(1) is obtained directly by first calculating the density $n_{0\sigma}(x)$ and the macroscopic velocity $\vec{v}_{0\sigma}(x)$ corresponding to a plasma whose guiding centers are located uniformly for $x > 0$ (for $x < 0$, there are no guiding centers) with a Maxwellian velocity distribution of the constant density and temperature. Then summing up these particle densities and velocities for $x=x_A$ and $x=-x_A$ ($x_A > 0$), one finds

$$n_\sigma^{LOM}(x) = n_{0\sigma}(x) + n_{0\sigma}(-x)$$

$$\vec{v}_\sigma^{LOM}(x) = \vec{v}_{0\sigma}(x) + \vec{v}_{0\sigma}(-x) \quad .$$

As illustrated in Fig.1-b, these currents appear because the currents due to the particles moving in a inversed magnetic field are not cancelled out but summed up with those coming from others missing the wall near the boundary.

It is to be noted that these currents resemble the diamagnetic currents due to the density gradient. Both are produced by the finiteness of the Larmor radius. Then these currents along the wall can cause a drift wave like instability if there is a small angle θ between the z-axis and the magnetic field (tilted B).

In order to verify the surface instability, we made a simulation using LOM boundary condition. A model we used is a 2 - 1/2 dimensional electrostatic dipole expansion code[11,12] with a static magnetic field slightly tilted from the z direction in the y direction. Finite size particles[13,14] with Gaussian shape charge distributions are used. The details of the system are shown in Fig.2. The plasma is uniform both in the x and y directions and is bounded by the conducting walls at x=0 and $x=L_x$ where the electrostatic potentials are zero. Periodic boundary conditions are used in the y direction; particles leaving a boundary at y=0 ($y=L_y$) are reintroduced at the opposite boundary at $y=L_y$ $(y=0)$. There are several choices for the treatment of the particles at the $x=0$ and $x=L_x$ walls. In this case, LOM boundary condition is used at the left wall $(x=0)$, while at the right wall $(x=L_x)$ Method I, which will be presented in Sec.3, is used. This is because if we use LOM for the both walls, there will be strong coupling of the waves excited at the each wall which confuses the diagnostics. Initially the guiding centers of the particles are uniformly loaded with Maxwellian velocity distributions. No quiet start technique[15] is used. The parameters are

System size,	$L_x \times L_y = 32 \times 32;$
Number of particles,	$N_e = N_i = 8192;$
Particle size,	$a_x = a_y = 1.5;$
Finite time step,	$\Delta t = 0.4;$
Mass ratio,	$m_i/m_e = 25;$
Temperature ratio,	$T_i/T_e = 0.25;$
Electron Debye length,	$\lambda_{De} = 1.41;$
Electron Larmor radius,	$\rho_e = 1.0;$
Ion Larmor radius,	$\rho_i = 2.5;$
Electron cyclotron frequency,	$\omega_{ce} = 1.41;$

Angle between the magnetic field and the z - axis, $\theta=1.5°$, where lengths and times are normalized by the grid spacing Δ and the inverse of the electron plasma frequency ω_{pe}, respectively.

Now, let us look at the gross behavior of the surface instability near the left wall. Fig.3 shows the time dependence of the Fourier components of the electrostatic potential, $(m,n)=(1,1)$, $(2,1)$ and $(3,1)$, where m and n correspond to the wave numbers, $k_x=m\pi/L_x$ and $k_y=2n\pi/L_y$. These modes grow above the thermal noise at $t\approx 800$, exponentiate linearly until $t\approx 1250$, saturate at $t\approx 1400$ and remain almost at the same amplitude after that (saturation stage). No instability is observed for n=2 and higher modes. The observed growth rate is $\gamma=0.0054$. Fig.3-b shows the time dependence of the phase of the mode $(m,n)=(2,1)$. Excellent coherency is observed after $t\approx 1000$ and the measured frequency from this is $\omega=0.0052$. The direction of phase velocity is that of the macroscopic electron velocity near the wall. This is confirmed by the other simulation using LOM at the right wall (at the left wall Method I is used), in which the direction of the phase velocity is changed corresponding to the change of the direction of the surface current.

The spatial structures of the n=1 mode are shown in Fig.4. The growth of the instability at the LOM boundary (x=0) is clearly observed. The width of the instability is about the ion Larmor diameter at the initial and middle stage of the linear growth (t=880 and t=1040). It begins to spread in the final stage of the linear growth (t=1280) and it is more than several times the ion Larmor radius in the saturation stage (t=1920). This spreading is crucial because simulation plasmas are usually $20\sim30\ \rho_i$ and there are two boundaries.

Fig.5 shows the spatial structures of the macroscopic currents due to the ions. In Fig.5-a which corresponds to the initial time of the simulation, there is a current near the left wall due to a special kind of the treatment of the particles by LOM. Its spatial dependence on x agrees quite well with the prediction of Eq.(1). At the initial stage of the linear growth (Fig.5-b), the surface currents are perturbed in the y direction due to the $\vec{E}\times\vec{B}$ drift by the n=1 surface mode. The width of the current is also about a ion Larmor diameter thick. At the final stage of the linear growth (Fig.5-c) the current is considerably modulated by the n=1 mode. Its width is about four times as large as the ion Larmor radius. The change of the current is due to the nonlinear transport of particles via $\vec{E}\times\vec{B}$ drift of the surface mode. The averaged x components of the currents is directed to the left wall, and this generates the large density gradient near the boundary. In the saturation stage (Fig.5-d) the width of the current layer further increases to more than several times ρ_i consistent with the structure of the n=1 mode. The form of the current layer is vortex like in this stage, and the initial current profile is almost completely wiped out.

Electron and ion temperatures which are parallel and perpendicular to the magnetic field are also observed. The result is the decrease of the electron parallel temperature near the left wall, which indicates the inverse Landau damping of the electrons as the origin of the instability.

From all the results described above, we know that this instability closely resembles the drift wave instability.[8,10] The parameters used here are also the ones that make the drift wave unstable if there is a density gradient. Hence if we make a drift wave simulation using LOM, the plasma will be unstable near the walls as well as in the density gradient region and these excited waves will be strongly coupled in the nonlinear stage of the instabilities. (We also verified this by the simulation.)

§3. Modifications of the boundary conditions

The surface instability produced by LOM has been verified in the previous section which is caused by the macroscopic current along the wall. It is clearly necessary to find a method which introduces no macroscopic currents or density gradients. In this section, we show such boundary conditions which cause no surface instability.

A. Method I

One of the methods we used is to reflect a particle with the reversed velocity (Method I, see Fig.1.c) at the wall

$$v_x \to -v_x \quad , \qquad v_y \to -v_y \tag{2}$$

where the coordinate system perpendicular to the magnetic field is assumed (the case of $\theta=0°$ in Fig.2). It is shown that there is no density gradients or macroscopic currents in this method using the analogous scheme described under Eqs.(1);

$$n_\sigma(x) = n_{0\sigma}(x) + n_{0\sigma}(-x) = \text{const.}$$
$$\vec{v}_\sigma(x) = \vec{v}_{0\sigma}(x) - \vec{v}_{0\sigma}(-x) = 0.$$

One must reflect only the components of velocity perpendicular to the magnetic field when one uses a 2 - 1/2 dimensional code (tilted B);

$$\begin{aligned} v_x &\to -v_x \\ v_y &\to -v_y \cos 2\theta + v_z \sin 2\theta \\ v_z &\to v_y \sin 2\theta + v_z \cos 2\theta \quad . \end{aligned} \tag{3}$$

Since the time is discretized in simulation, one should determine the new position of a particle using linear interpolation

$$\begin{aligned} x &\to 2x_0 - x \\ y &\to r(y_- - v_x \Delta t) + (1 - r) y \\ r &= (x - x_0)/(x - x_-) \end{aligned} \tag{4}$$

where x_0, x_-, y_- represents the position of the wall and the x and y coordinates of a particle before pushing, and the other values appearing at the right hand sides of the equations are the values before reflection. Eqs.(4) can be used both for the 2 and 2 - 1/2 dimensional codes.

One may think that the guiding center shifts at the wall inherent to Method I would dominate the physics (perhaps this motivated LOM and the method used by W. Nevins and M.J. Gerver[6]). However what is important is the macroscopic currents to which the particles which just miss the wall contribute as well as those which hit the wall.

Method I have been used at the right wall ($x=L_x$) of the system in the simulation which is presented in the previous section. Fig.5-a shows that initially there is no macroscopic current at the right wall. Fig.4 and Fig.5-b~d indicate that there is no surface instability at the right wall. From these figures, Method I is shown to be useful because it actually doesn't influence the surface instability excited at the left wall; the surface instability due to LOM is successfully simulated without suffering no disturbance from the right wall. This method has been used quite satisfactorily in the simulation studies of the drift wave instabilities caused by the density and the temperature gradients.[16]

B. Method II

As indicated in Method I, if we could choose the initial condition correctly, the currents caused by the guiding center shifts of the particles which hit the walls and those caused by particles which never hit the walls would cancel out. Then there would be no macroscopic currents even for the case of reflecting boundary conditions. We show below one such initial condition; (1) First the guiding centers of the particles are uniformly loaded in the system and the real velocities are assigned to those, (2) second the real positions of the particles are determined from (1) and if they are outside the boundary, the positions and the velocities of the particles are changed as

$$\begin{aligned} x &\to 2x_0 - x \\ v_x &\to v_x \\ v_y &\to -v_y \ . \end{aligned} \tag{5}$$

where new guiding centers of these particles are outside the boundary. (see Fig.1-d). In the 2 - 1/2 dimensional code, v_y and v_z should be changed following the last two equations of Eqs.(3), while x and v_x should be changed following Eqs.(5).

Method II uses this initial condition with the reflecting boundary condition. Note that this initial condition is the one that should be used with Method I. To prove that there are no surface currents and density gradients in Method II, let us show Method I and II are the same macroscopically. As is illustrated in Fig.6, a particle $P_1(P_1')$ and a particle $P_2(P_2')$ moves differently according to the Method I and II, respectively. However, there are many particles on the orbits a, b, c, d and the initial particle distributions on these orbits are uniform and the same statistically. Then the total current and density contributions from these particles are the same macroscopically. The initial condition in Method II is not unique and one can use many other choices, if one wants to reduce the statistical fluctuations.

The simulation is made using Method II with the same system and parameters described in Sec.2. It is found that there is no density gradients or surface currents and that there is no surface instabilities. Additional simulation is done using another incorrect initial conditions ($v_x \to -v_x$ $x \to 2x_0 - x$) with reflecting boundary conditions. As pointed out by Lee and Okuda[5] and described in Sec.2, it is found that there are large density gradients and macroscopic currents. These effects are produced by the change in the probabilities of the particle distributions on orbit c and d in Fig.6-b due to the incorrect initial conditions. All the guiding centers of the particles are inside the system. It is also to be noted that the dominant surface current in this case is not due to the guiding center shifts of the particles which hit the walls but due to the particles which miss the walls (,viz, due to diamagnetic current).

The results using Method II is consistent with the fact that fully ionized plasma confined by perfectly reflecting walls has no magnetic effect at all, if a plasma is in thermodynamic equilibrium.[17] But the method to realize this thermodynamic equilibrium state in a bounded simulation plasma using uniform guiding center loadings have not ever been used before. If the real positions of the particles are uniformly loaded this state is also realized, but then the benefit of using uniform guiding center loadings will disappear and there will be considerable fluctuations.

C. Random reflection method

There is another set of boundary conditions where particles are reflected with given velocity distribution. In the unmagnetized plasma, particles are reintroduced with a half-Maxwellian velocity distribution.[7] However in the magnetized plasma we have the velocity distributions as

$$f_\sigma(v_x) = \sigma_j (|v_x|/v_{t\sigma}{}^2)\exp(-v_x{}^2/2v_{t\sigma}{}^2)$$

$$f_\sigma(v_y) = (1/\sqrt{2\pi}\ v_{t\sigma})\exp(-v_y{}^2/2\ v_{t\sigma}{}^2) \tag{6}$$

where

$j = R, L$

$\sigma_R = -1 \quad , \quad \sigma_L = 1$

where subscripts R and L represents the left and right walls, respectively. Eqs.(6) are obtained by calculating the velocity distribution of particles which cross the wall $x=x_0$ in the +y (-y) direction assuming a homogeneous plasma whose guiding centers are located uniformly in the whole space with a Maxwellian velocity distribution. Because the energetic particles have larger Larmor radius than the cold particles, large number of energetic particles can cross the wall at $x=x_0$. This produce a change in a velocity distribution described above.

One must use the linear interpolations to determine the new position as

$$x \to x_0 + r\, v_x^N \Delta t$$

$$y \to r(y_- + v_y^N \Delta t) + (1-r)y \quad , \qquad (7)$$

where v_x^N and v_y^N are the new velocities according to Eqs.(6) and r is the same as the one appearing in Eqs.(4). It is straightforward to extend Eqs.(6) and (7) to the 2 - 1/2 dimensional code. We also checked this method and there are no density gradients or surface currents. When the linear interpolations in Eqs.(7) are not used, however, the density gradients and surface currents become large as the time steps increase.

D. Nevins and Gerver's Method

Let us see the method used by Nevins and Gerver (we call this NGM)[6] to compare it with methods described earlier. In NGM they use an assumption that the plasma has inverse symmetry around the point (x=0, y=0). (The region to be used is $0 < x < L_x$, $-L_y/2 < y < L_y/2$.) Then a particle going out of the x=0 boundary at $y=y_0$ is reintroduced at $y=-y_0$ and x=0, with its velocity (x, y, z component) reversed. This hold both for the 2 and 2 - 1/2 dimensional codes. NGM has no instability near the wall because there is no current or density gradient. However, the boundary condition for the field are rather complicated as shown in Ref.6. There may be some connection of the upper (y>0) and lower (y<0) domain by wave packets propagating in the x direction in the nonlinear stage of the drift wave instability (They developed NGM for drift wave simulations). Furthermore we can't use NGM when we want to simulate the boundary phenomena, because NGM is equivalent to having no wall at all at x=0.

Compared with LOM and NGM, Method I, Method II and random reflection method are simple and straightforward and make no artificial assumption. They are better than LOM because there is no surface current or surface instability. They are also better than usual reflecting boundary condition because there is no density gradients which produces large electric field near the boundary due to the differences in gyroradii between electrons and ions.

§5. Discussions and Conclusions

In this paper, we studied different treatments of the particles at the boundary in a magnetized and bounded simulation plasma. It is found that Lee and Okuda's boundary condition introduces the macroscopic currents near the boundary which cause drift wave like surface instability. This is verified by the numerical simulations. Moreover it is found that this surface instability affects the interior of the plasma because it spreads over a distance which is more than several Larmor radius.

We describe three methods (Method I and II and the random reflection method) to treat the particles at the walls. They are simple and straightforward and introduce no density gradients or macroscopic currents, and hence introduce no surface instability. We also verified this by the simulations. In Method I particles are reflected with inverse velocities which are perpendicular to a magnetic field. Method II changes the initial loadings of the particles correctly with the usual reflecting boundary conditions. These two method are shown to be identical macroscopically. In random reflection method particles are reflected with a new velocity distribution which are different from a half-Maxwellian velocity distribution due to the existence of the magnetic field.

When we use a bounded plasma model to simulate the phenomena in the interior of the system, Method I will be suitable. However when we want to simulate the boundary phenomena, Method II may be more realistic. Random reflection method can be used for the aims such as fixing the temperature at the walls.

It is to be noted that surface currents disturb the interior of the plasma only after the time when the instability occurs in the electrostatic code. However in the magnetostatic code[18] this surface current itself can influence the external magnetic field and plasma will be strongly dismagnetic. The phenomena we want to simulate will considerably change. Our methods are useful not only for the 2 and 2 - 1/2 dimensional electrostatic code verified in this paper, but these will be also useful for the 3 dimensional electrostatic code or the magnetostatic particle simulation code.

Acknowledgements

The authors gratefully acknowledge Professor J.M. Dawson and Dr. Y. Ohsawa for helpful discussions and suggestions. They are also grateful to Professor A.K. Sen for his critical reading of this manuscript and to the members of the computer center of the Institute of Plasma Physics, Nagoya University, for their assistance with the computer simulations.

References

1) H. Okuda and J.M. Dawson, Phys. Fluids 16, 408 (1973)

2) C. Chu, J.M. Dawson and H. Okuda, Phys. Fluids 18. 1762 (1975)

3) R.W. Gould and A.W. Trivelpiece, in "Proceedings of the Symposium on Electronic Wave-guides", Polytechnic Press, New York, 215 (1958); A.W. Trivelpiece and R.W. Gould, J. Appl. Phys. 30, 1784 (1959)

4) V.K. Decyk and J.M. Dawson (to be published)

5) W.W. Lee and H. Okuda, (to be published in J. Comp. Phys.), Princeton Plasma Physics Laboratory MATT Report #1231 (1976)

6) W. Nevins and M.J. Gerver, in "Second quarter progress report on plasma computational research", July 1, (1976), University of California

7) A.B. Langdon and B.F. Lasinski, in "Methods in Computational Physics" 16, 327 (1976)

8) W.W. Lee and H. Okuda, Phys. Rev. Letters 36, 870 (1976)

9) M. True, W.W. Lee and H. Okuda, Princeton Plasma Physics Laboratory MATT Report #1270 (1976)

10) C.Z. Cheng and H. Okuda, Phys. Rev. Letters 38, 708 (1977)

11) W.L. Kruer, J.M. Dawson and B. Rosen, J. Comp. Phys. 13, 114 (1973)

12) T. Kamimura, J.M. Dawson, B. Rosen, G.J. Culler, R.D. Levee and G. Ball, UCLA Report PPG-248, (1975)

13) A.B. Langdon and C.K. Birdsall, Phys. Fluids 13, 2115 (1970)

14) H. Okuda and C.K. Birdsall, Phys. Fluids 13, 2123 (1970)

15) J.A. Byers and M. Grewal, Phys. Fluids 13, 1819 (1970)

16) S. Tokuda, T. Kamimura and H. Itoh, (in preparation)

17) T.G. Cowling, M.N.R.A.S. 90, 140 (1929)

18) C.W. Nielson and H. Ralph Lewis, in "Methods in Computational Physics" 16, 367 (1976)

Figure Captions

Fig.1 Illustrations for different boundary conditions. Reflecting boundary condition is shown in (a). Lee and Okuda's method is shown in (b). The origin of the surface current in this method is also shown. Method I is shown in (c). Initial condition in Method II is shown in (d) where x_0 indicates the position of the wall. It shows the initial treatment of the particles which are outside the system due to the uniform loadings of the guiding centers. The combination of this initial condition and the reflecting boundary condition is Method II. Note that this initial condition is the one used in Method I.

Fig.2 Sketch of the bounded plasma model in a magnetic field. The case of the $\theta=0°$ and $\theta\neq0°$ correspond to the 2 and 2 - 1/2 dimensional code, respectively. Periodic bourdary condition is used in the y direction.

Fig.3 (a) Growth of Fourier modes of the electrostatic potential.

(b) Phase of the mode $(m,n)=(2,1)$.

Fig.4 Mode structures for n=1 mode, The growth of the mode is shown in conjunction with the spreading of the width of the instability. Lee and Okuda's boundary conditions are used at the left wall, while at the right wall Method I is used.

Fig.5 Spatial structures of the macroscopic currents due to the ions. The lengths of the arrows are proportional to the magnitudes of the currents. One fourth of the L_x is equal to the magnitude $n_0 v_{ti}$. Each figure corresponds to (a) the initial time of the simulation, (b) the time when instability sets in, (c) the final stage of the linear growth and (d) the saturation stage of the instability.

Fig.6 Illustration that (a) Method I and (b) Method II are macroscopically same.

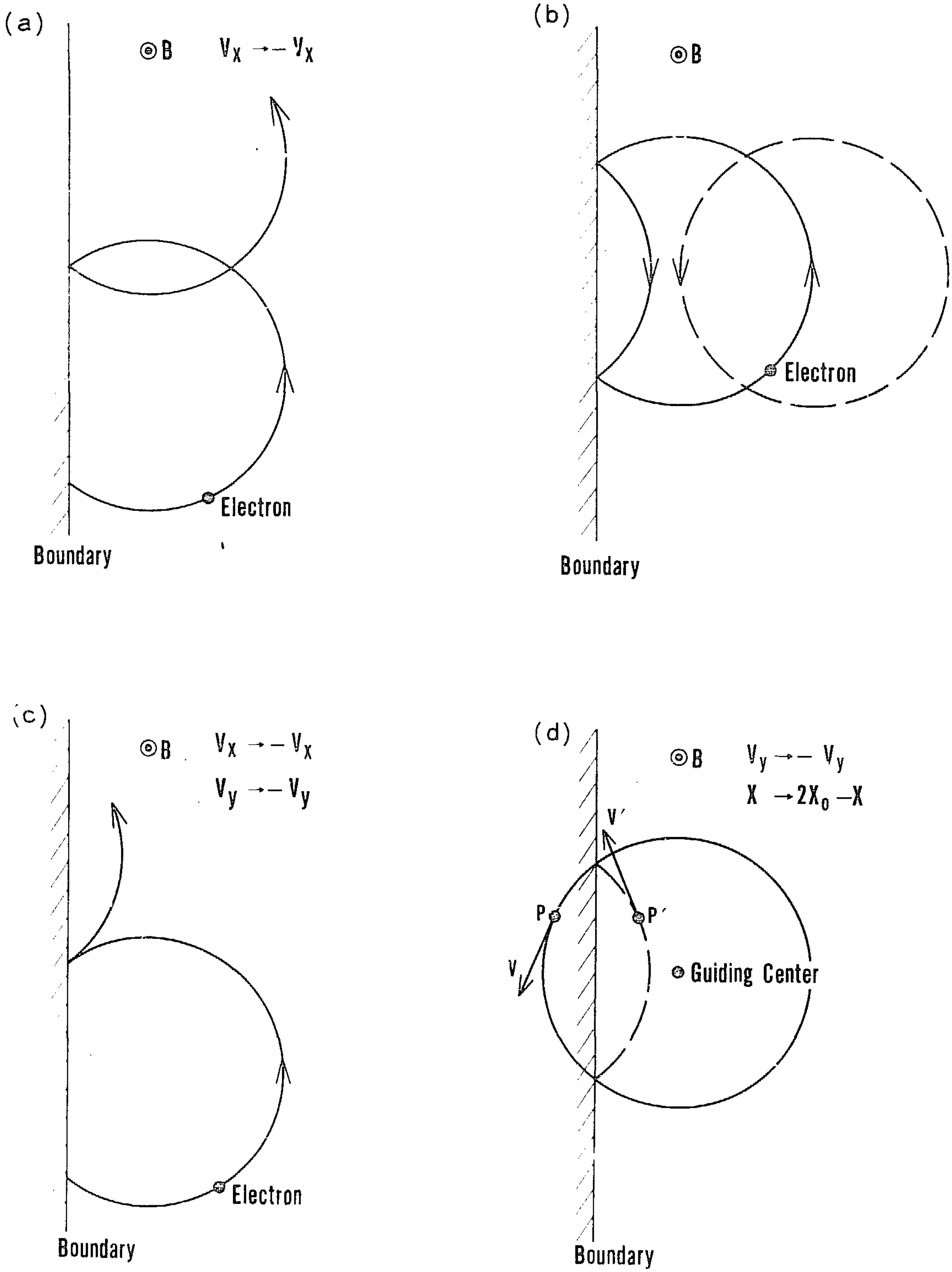
(a)
⊙B
V_X → − V_X
Electron
Boundary
(b)
⊙B
Electron
Boundary
(c)
⊙B
V_X → − V_X
V_y → − V_y
Electron
Boundary
(d)
⊙B
V_y → − V_y
X → 2X_0 − X
V′
P
P′
V
Guiding Center
Boundary

Fig. 1

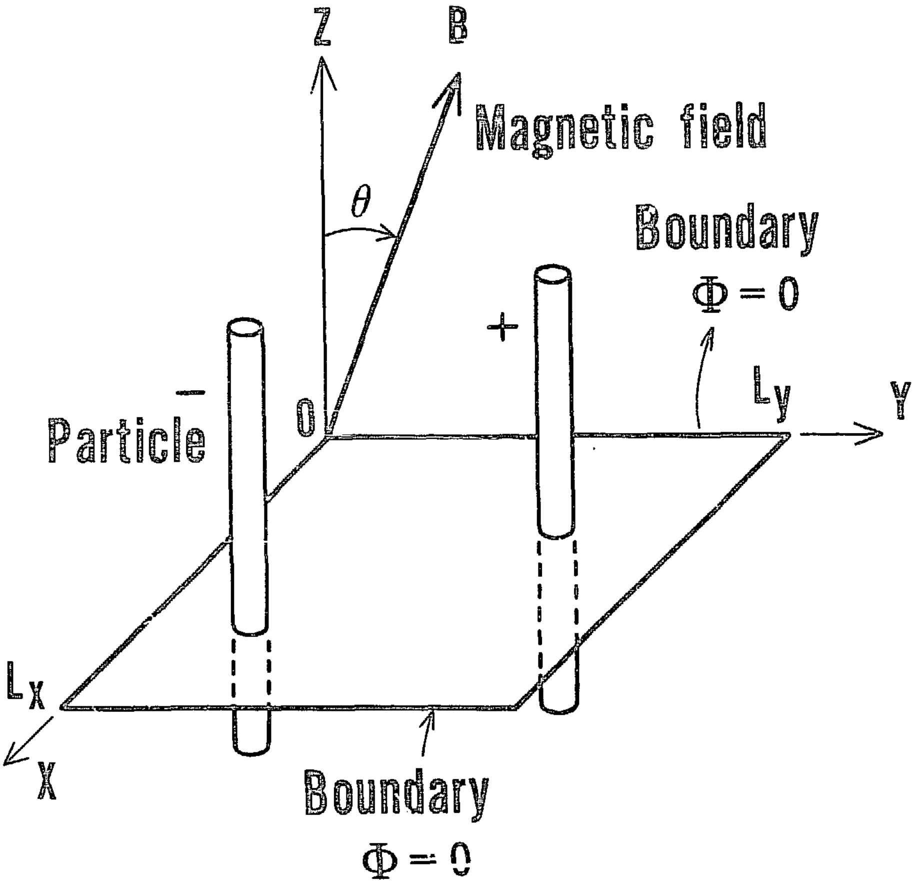

Z
B
Magnetic field
θ
Boundary
Φ = 0
+
−
Particle
O
Ly
Y
Lx
X
Boundary
Φ = 0

Fig. 2

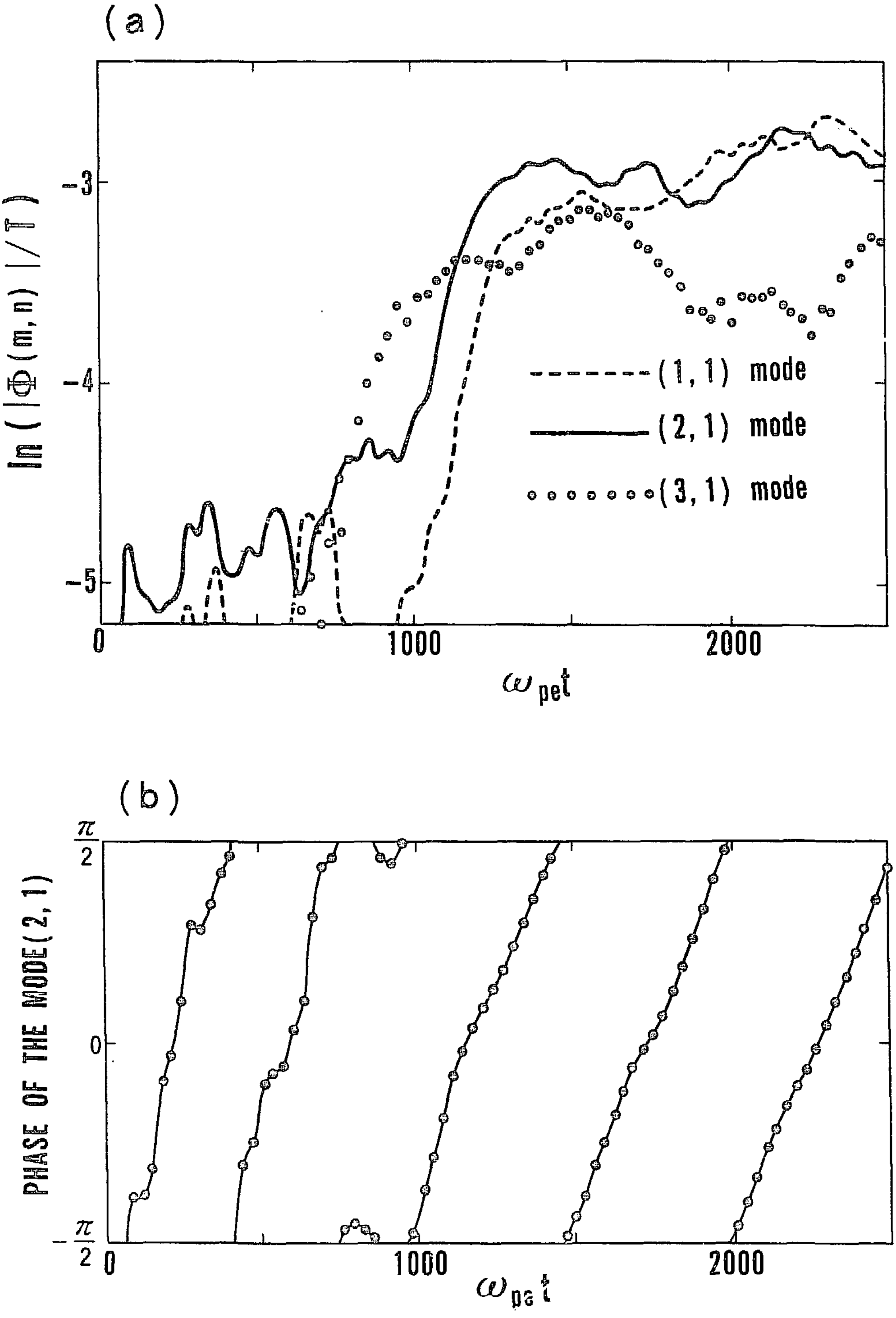

(a)
ln (|Φ(m, n)| / T)
-3
-4
-5
0
1000
2000
$\omega_{pe}t$
(1, 1) mode
(2, 1) mode
(3, 1) mode
(b)
PHASE OF THE MODE (2, 1)
$\frac{\pi}{2}$
0
$-\frac{\pi}{2}$
0
1000
2000
$\omega_{pe}t$

Fig. 3

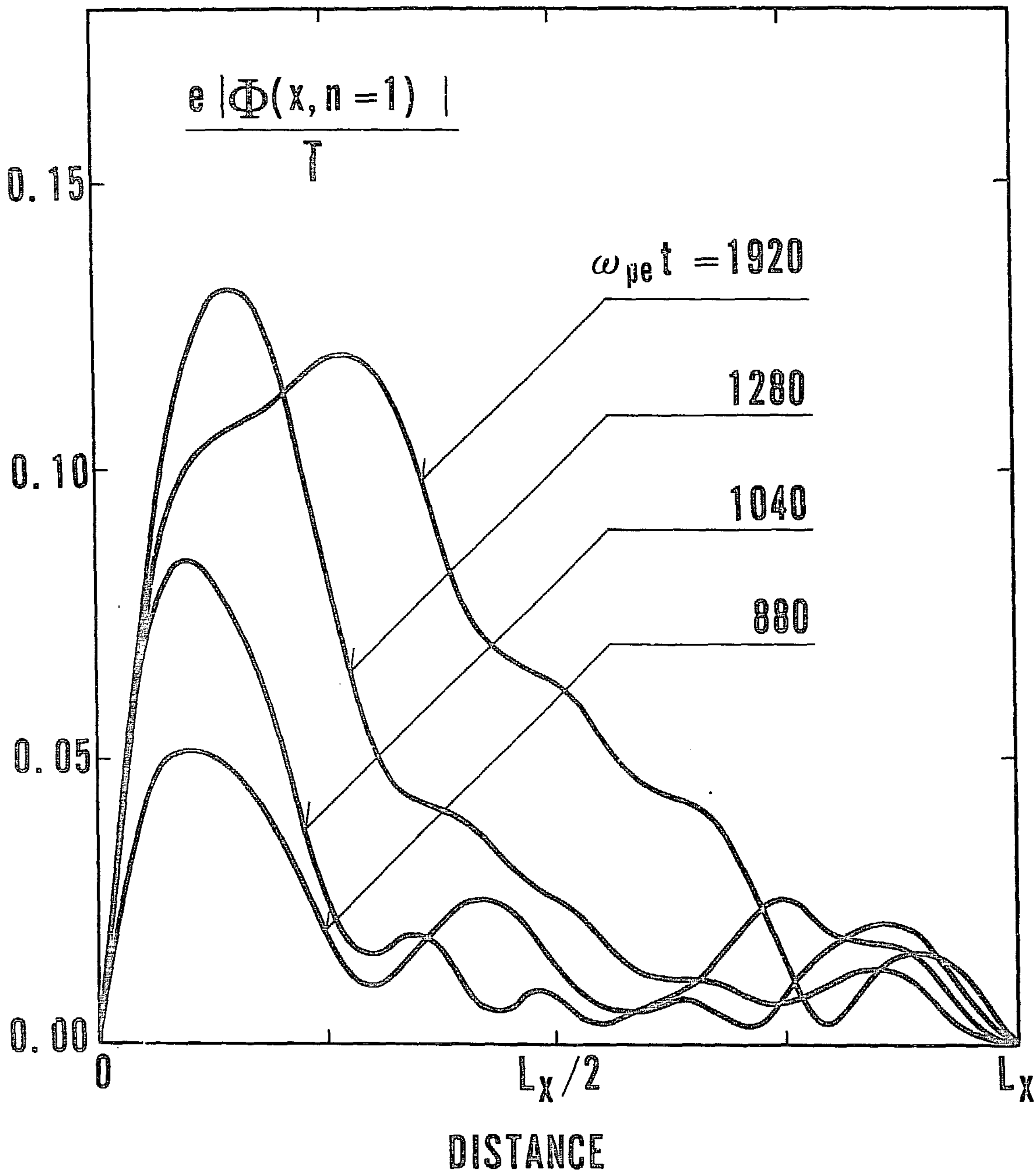

$\frac{e|\Phi(x, n=1)|}{T}$
0.15
0.10
0.05
0.00
$\omega_{pe}t$ = 1920
1280
1040
880
0
$L_x/2$
L_x
DISTANCE

Fig. 4

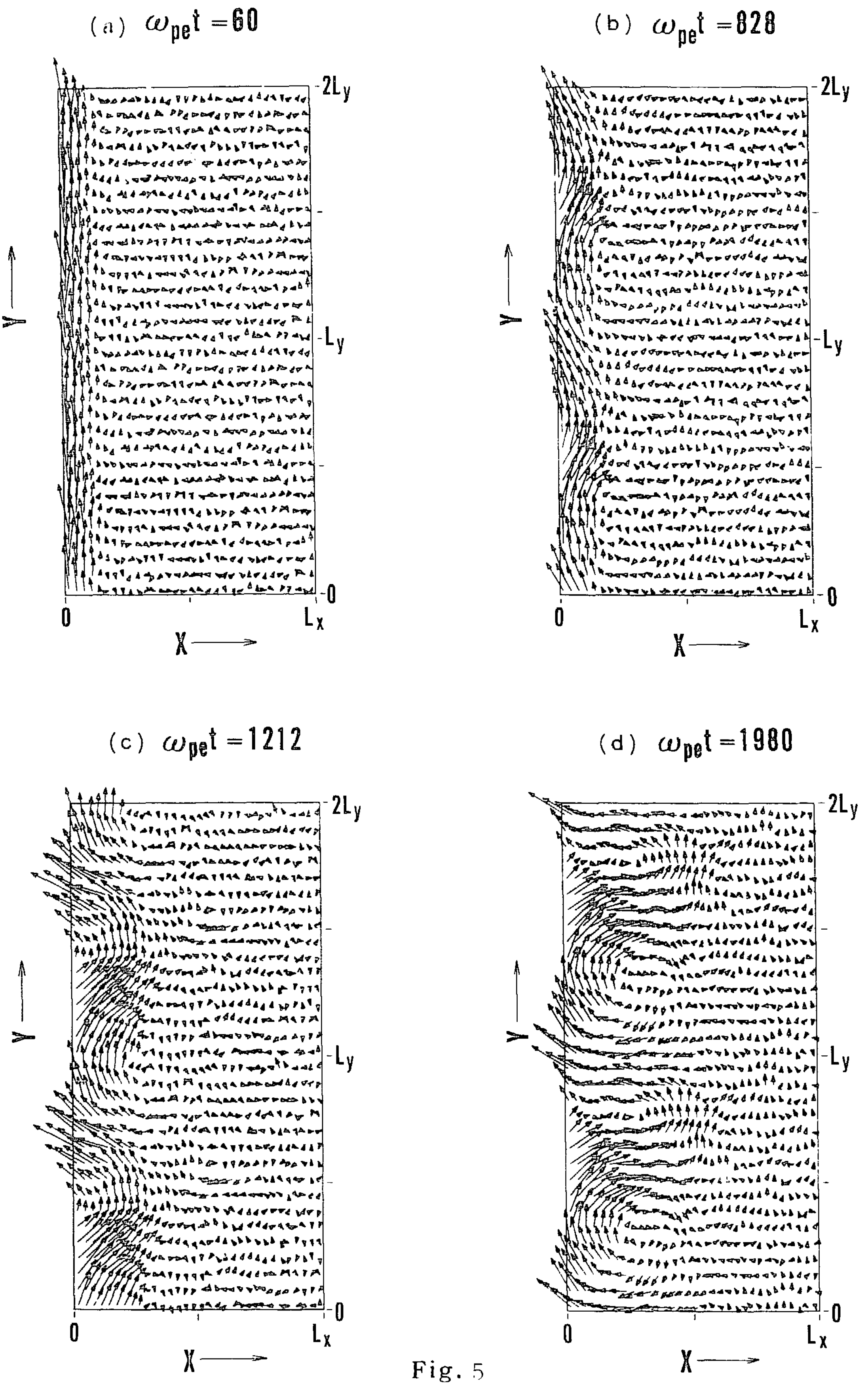
(a) $\omega_{pe}t = 60$
(b) $\omega_{pe}t = 828$
(c) $\omega_{pe}t = 1212$
(d) $\omega_{pe}t = 1980$
2Ly
Ly
0
Lx
Y
X

Fig. 5

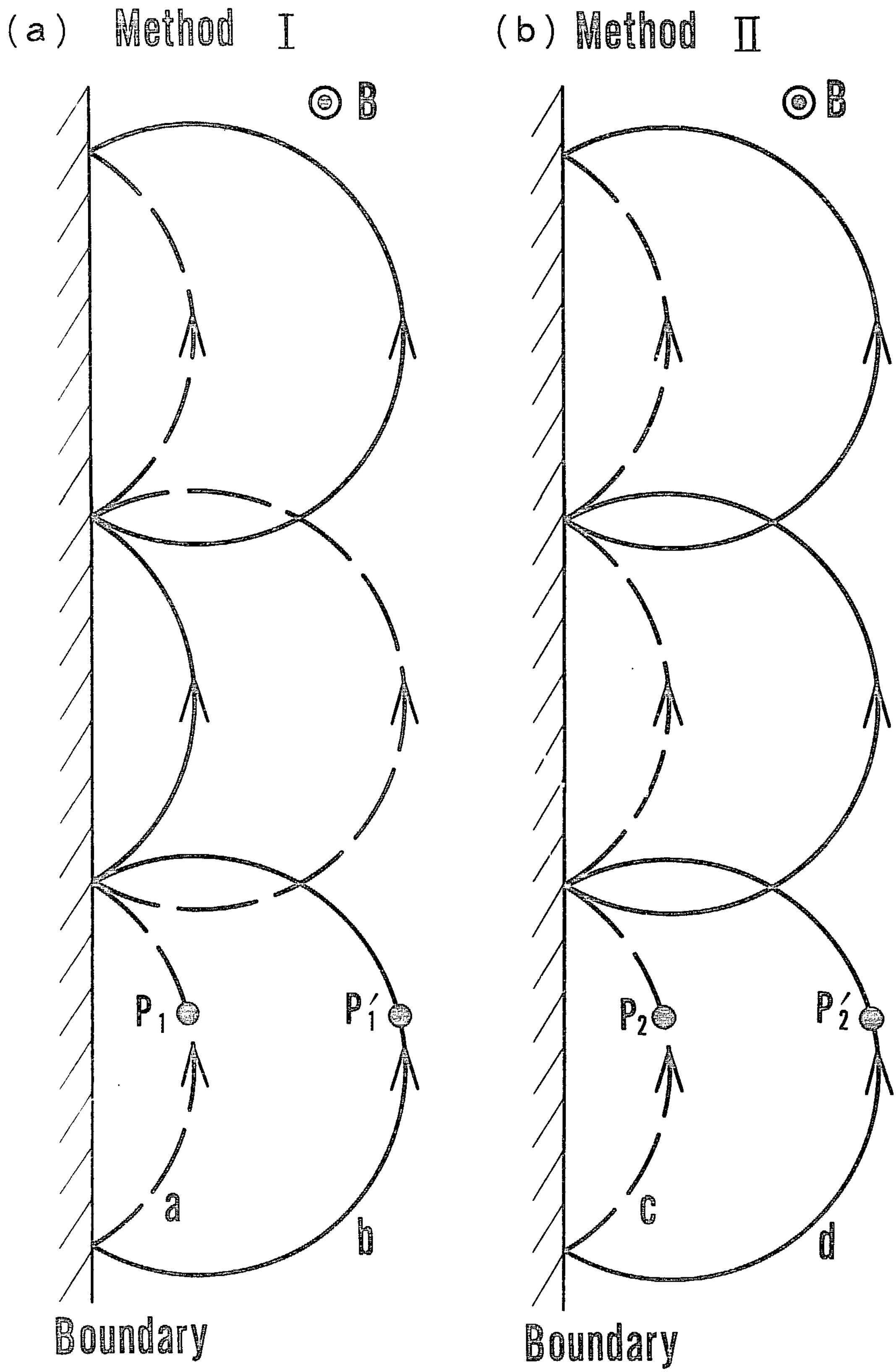

Fig. 6